Proceedings of the XVII ECSMGE-2019
Geotechnical Engineering foundation of the future
ISBN 978-9935-9436-1-3

doi: 10.32075/17ECSMGE-2019-0846

Research on the horizontal bearing capacity of BFRP pile

Recherche sur la capacité portante horizontale des pieux BFRP

Yang Yang

Southeast University, Nanjing, China

Weiming Gong, Kang Zhou, Guoliang Dai

Southeast University, Nanjing, China

ABSTRACT: This paper reports on the experimental results of low-cyclic reversed loading test on Basalt Fiber-Reinforced-Polymer (BFRP) pile to study the character of horizontal bearing capacity of the specimen using a new fiber material with lower density, high strength and corrosion resistance. The stiffness degeneration, ductility and energy dissipation principle of BFRP pile were summarized. The results show that in the experiment there is no cracks on BFRP tube and the damage of BFRP pile and the decrease of bearing capacity happened suddenly with no plane and downward part of skeleton curve which means the distortion of BFRP pile is obvious. Limit bearing capacity, limit displacement, energy dissipation coefficient and displacement ductility of BFRP pile is obtained in the experiment.

RÉSUMÉ: Cette dissertation montre les résultats expérimentaux d'un essai de charge inversée à faible cyclisme sur un pieu en polymère renforcé de fibres de basalte (BFRP) afin d'étudier le caractère de la capacité portante horizontale de l'éprouvette à l'aide d'un nouveau matériau fibreux de densité plus faible, de résistance élevée et de résistance à la corrosion. Les principes de dégénérescence de rigidité, de ductilité et de dissipation d'énergie du pieu BFRP ont été résumés. Les résultats présentent que, dans l'expérimentation, il n'y a pas de fissure sur le tube BFRP et que l'endommagement du pieu BFRP et la diminution de la capacité portante se sont produits soudainement sans aucune partie plane et descendante de la courbe du squelette, ce qui signifie que la distorsion du pieu BFRP est évidente. La capacité portante limite, le déplacement limite, le coefficient de dissipation d'énergie et la ductilité du déplacement du pieu BFRP sont obtenus dans l'expérimentation.

Keywords: BFRP pile; Horizontal bearing capacity; Low-cyclic reversed loading test

1 INTRODUCTION

Durability has a great effect on the quality of pile foundation and the corrosion environment aggravates the degradation of pile bearing capacity, the generation of additional settlement and differential settlement, etc., result in massive expenses of repairment and replacement in the future. Fiber-Reinforced-Polymer (FRP), a new high-performance composite material has emerged since 1980s (Zhu et al. 2015). The application of FRP in pile foundation engineering can significantly improve the durability of foundation. The commonly used FRP composite pile is to inject concrete into FRP pipe with or without steel cage.

Fam et al (2001) have studied the behavior of axially loaded circular concrete columns confined by FRP tubes and proposed its analytical model. It was found that the central hole size and axial loading can reduce the confinement and the stiffness of the tube improves the effect. Frost et al (1999) has researched behavior of interfaces between fiber-reinforced polymers and sands. Mirmiran et al (2002) has studied piles under pile driving impact and it was similar with the prestressed-concrete piles. Pando et al (2002) tested the properties of FRP composite piles under lateral load finding the load-displacement characteristics was similar with prestressed-concrete piles. Murugan et al (2017) studied fiber-reinforced polymers piles, glass fiber-reinforced polymers and carbon fiber-reinforced polymers piles under cyclic lateral loads. Weaver et al. (2008) conducted full-scale lateral load tests of a concrete-filled glass-fiber reinforced polymer pipe pile. Ramaswamy et al. (2014) studied the performance of basalt fiber reinforced polymer composites retrofitted RCC piles under axial loads finding the improvement of axial compression performance. BFRP is a new material different from the common used Carbon Fiber Reinforced Plastics (CFRP) and Glass Fiber Reinforced Polymer (GFRP) materials, the research results are difficult to be applied to the research and design of BFRP piles directly, and the bearing capacity of BFRP piles needs further studies.

In the design of pile foundations for structures such as large wharfs, river-crossing and sea-crossing bridges and off-shore oil production platforms, the effect of horizontal cyclic loads such as waves or earthquakes on the pile foundations must be considered. Therefore, the study on the mechanical properties of BFRP piles under laterally cyclic load has significant engineering value. Therefore, laterally cyclic load tests of BFRP pile was carried out to analyze the failure phenomena, stiffness degradation, ductility performance and energy dissipation performance.

2 EXPERIMENTAL PROGRAM

2.1 Material properties and parameters

The test was carried out on one BFRP pile, a concrete-filled BFRP pile with 4 hot-rolled plain steel bars. The diameter of the steel bars is 16 mm and the standard value of yield strength is 400MPa. At the same time of making the specimen, three concrete blocks with the side length of 100mm were casted in the same batch of concrete for testing the compressive strength of the concrete cube and three concrete blocks with the side length of 150mm were poured for testing the axial compressive strength of the concrete, the test results are shown in Table 1. BFRP properties and BFRP pile properties are shown in Table 2 and Table 3, respectively.

Table 1. Concrete properties

Side length /mm	Compressive strength /MPa
100	33.7
150	22.6

2.2 Test setup and instrumentation

The vertical loading device is composed of a reaction beam, an electro-hydraulic servo loading system and a uniformly loaded steel plate. The experimental photos are shown in Figure 1.

This test adopts displacement control. This test adopts displacement control.Before the formal test, the pre-loading was carried out twice, with the positive and negative pre-loading values of 10kN respectively. This procedure can check whether all the test instruments were working normally, squeeze out the tiny gap between the test device and the pile, and tighten the bolts. After confirming that the instruments are normal, the 10kN load is removed and the formal loading begins after a period of stabilization.The formal loading was controlled by the displacement of the pile. The displacement value of each stage was increased by 5mm in positive and negative direction, and the displacement of each stage was repeated for three times.When the bearing capacity of the pile drops to 85% of the maximum bearing capacity, the loading is stopped.

(a)Positive loading

(b) Negative loading

Figure 1. Experimental photos

This test adopts displacement control. The displacement meters were arranged symmetrically on both sides of the pile to monitor the displacement of the pile midspan. In order to accurately grasp the strain distribution of concrete, a total of 8 concrete strain gauges were set in the pile body with equal spacing, 30cm from span, as shown in the following Figure 2.

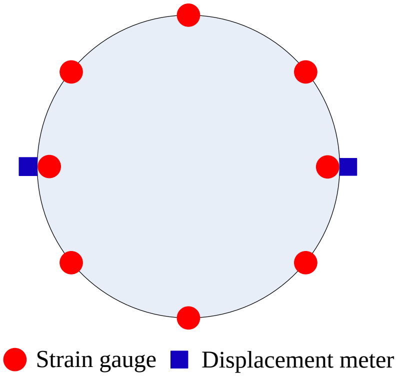

Figure 2. Layout of the measurement points

3 TEST RESULTS AND OBSERVATIONS

3.1 Test results

It is specified that the positive displacement is downward. When the positive and negative displacement reaches to 10mm, the corresponding force is 70.33kN and 65.22kN, respectively. No cracks appeared on the surface of the basalt fiber, and the deformation of the specimen loading became lager with the load.

When the positive displacement reached to 140mm, the force induced by the displacement reached to 554kN, and the bearing capacity did not decline. When the reverse displacement reached to 140mm, the force reached to 592kN, and the mid-span basalt fiber cracked, the bearing capacity suddenly decreased and the test ended. Because of the excellent properties of BFRP, no cracks appeared on the surface of the material before destruction.

3.2 Observations

As the inner concrete was wrapped by the BFRP tube, the cracks of core concrete are difficult to be observed directly. It is necessary to split the surface of tube after the end of the test to observe the cracks of core concrete. In order to further study the characteristics of concrete, steel bars and BFRP tube, the BFRP tube was split to observe the cracks of concrete and the failure forms of BFRP tube and steel bars. The specimens deformation and BFRP failure model are shown in Figure 3.

There was a 3cm crack in the concrete mid-span, indicating that the concrete had completely lost its bearing capacity at the later stage of loading and the steel bar in the span was exposed. The crack is distributed approximately symmetrically by taking the mid-span as the axis of symmetry. The farthest distance of one side of the crack is 110cm, and the farthest distance of the other side is 140cm. Based on the concrete damage situation, the BFRP specimen with a tube wall thickness of 25mm can still bear the load when the steel bars and concrete completely lose the bearing capacity, which indicates the excellent mechanical properties of the BFRP, and also indicates that the tube wall thickness need further studied.

BFRP tube was made of multiple fiber layers, which have 3 different arrangement direction respectively including axial, radial, and canted 45 ° direction, as shown in Figure 3(c), thus there are different mechanical properties between the BFRP and BFRP tubes. The inner surface of BFRP tube is smooth, and the surface of core concrete is smooth, as shown in Figure 3(d). Therefore, the adhesive strength of BFRP tube and concrete is low without measurements to increase the bond strength such as using thread, cementation and shear keys.

(a) *Split BFRP pile photo*

(b) *Crack in the mid-span* (c) *Failure of the BFRP tube in the mid-span* (d) *Smooth bonding surface*

Figure 3 Failure of specimens

4 DISCUSSION

4.1 Hysteretic curves and skeleton curves

Hysteretic curve is used to analyse the components' deformation capacity, stiffness degradation and energy dissipation performances [9]. Based on the measured load-displacement relationship in the test, the hysteresis curve of the pile is drawn, as shown in Figure 4.

The skeleton curve is a reflection of the mechanical characteristics of components in terms of stiffness, ductility and energy dissipation at different loading stages, as shown in Figure 5. The skeleton curve of BFRP pile is approximate to a straight line. As the load increases, the slope decreases slightly. The mid-span displacement, force induced by positive load and force induced by negative load at failure point are 140mm, 592.07kN and 553.72kN, respectively.

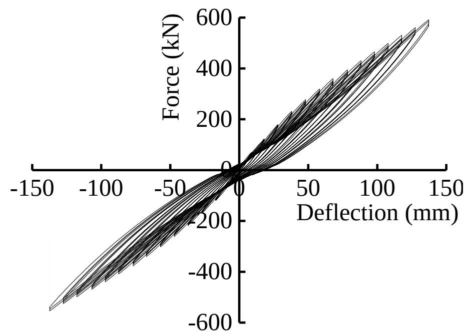

Figure 4 Hysteresis curve

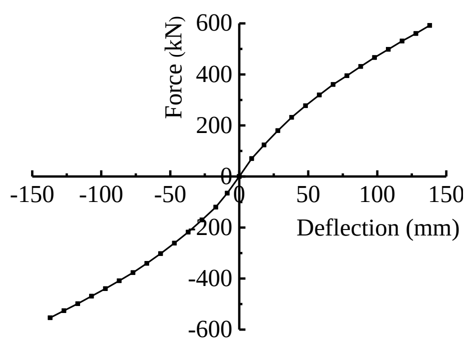

Figure 5 Skeleton curve

4.2 Strength and stiffness degradation

The maximum and minimum values of the BFRP pile's degradation coefficient of bearing capacity under each displacement amplitude are 0.976 and 0.966, respectively, which means the BFRP pile has basically no strength degradation under low cyclic repeated loading. The stiffness degradation curve of the specimen is shown in Figure 6.

Figure 6 shows that the initial stiffness of BFRP pile is relatively low, and the stiffness value decreases with the increasing of displacement, meaning that the stiffness degradation phenomenon occurs. The slope of the curve gradually decreases, indicating that the stiffness degradation is faster in the early stage of loading, and the rate of stiffness degradation slows down with the increasing of displacement. When the displacements are 10mm and 140mm the stiffnesses are 7.65kN /mm and 4.16kN /mm, respectively.

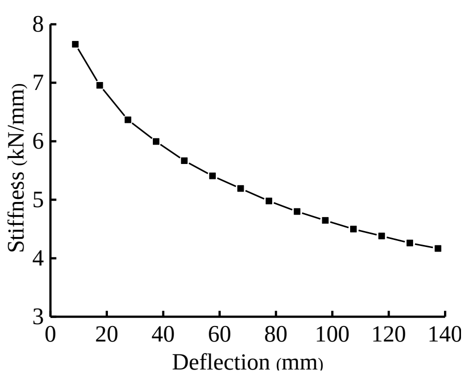

Figure 6 Stiffness degradation curve

4.3 Ductility and energy-dissipation

The load-displacement curve of non-ideal elastoplastic members has no obvious inflection point, and the yield displacement is difficult to be determined by the figure. The yield displacement is determined through the geometric mapping method and the energy equivalence method [10], and the displacement ductility factor is shown in Table 4.

The energy dissipation coefficient of the loading state at the first stage before the failure is taken, and the hysteresis loop of the pile under the loading state at the first stage before the failure is shown in Figure 7. The calculation results of energy dissipation coefficient are shown in table 5.

The skeleton curve of BFRP pile is not satiable, and the energy dissipation coefficient is significantly low, which is deficient in energy dissipation.

Table 4. Displacement ductility factor

Method	Yield displacement /mm	Ultimate displacement /mm	Displacement ductility factor
Geometric mapping method	100.25	140	1.38
Energy equivalence method	116.34	140	1.19

Table 5. Energy dissipation coefficient

Area of hysteresis loop /mm^2	Area of two triangle /mm^2	Energy dissipation coefficient (E)
12959	78738	0.165

5 CONCLUSIONS

(1) BFRP pile did not have cracks on the surface of BFRP tube in the test. After large deformation, it suddenly broke and damaged, and its bearing capacity suddenly decreased. There was no parallel descending section and yield point in the skeleton curve, which was characteristic of ductile failure.

(2) The ultimate bearing capacity of BFRP pile is high when it is damaged, the elastic modulus of BFRP pile is small, and the limit displacement is large when it is damaged. Therefore, new criteria and criteria should be formulated for the destruction of BFRP pile.

(3) The bearing capacity degradation coefficient of BFRP pile is greater than 0.9 under low cyclic repeated loading, and the strength degradation is not obvious. The slope of the stiffness degradation curve is low and the stiffness degradation is not obvious.

(4) Under the serviceability limit state, BFRP piles are less energy-consuming than traditional concrete piles.

6 ACKNOWLEDGEMENTS

The authors would like to express their special thanks and gratitude to the National Natural Science Foundation of China (51478109, 51678145).

7 REFERENCES

Zhu, H., Dong, Z. Q., Wu, G. 2015 Experimental study and theoretical calculation on the flexural stiffness of concrete beam reinforced with FRP bars, *China Civil Engineering Journal* **11**, 44-53.

Fam, A. Z., Rizkalla, S. H. 2001. Confinement model for axially loaded concrete confined by circular fiber-reinforced polymer tubes, *Structural Journal* **98**, 451-461.

Frost, J. D., Han, J. 1999. Behavior of interfaces between fiber-reinforced polymers and sands, *Journal of geotechnical and geoenvironmental engineering* **125**, 633-640.

Mirmiran, A., Shao, Y., Shahawy, M. 2002. Analysis and field tests on the performance of composite tubes under pile driving impact. *Composite Structures* **55**, 127-135.

Pando, M. A., Filz, G. M., Dove, J. E., Hoppe, E. J. 2002. Interface shear tests on FRP composite piles. *In Deep Foundations 2002: An International Perspective on Theory, Design, Construction, and Performance*, 1486-1500.

Murugan, M., Muthukkumaran, K., Natarajan, C. 2017. FRP-Strengthened RC Piles. II: Piles under Cyclic Lateral Loads. *Journal of Performance of Constructed Facilities* **31**, 04017004.

Weaver, T. J., Ashford, S. A., Rollins, K. M. 2008. Lateral Load Behavior of a Concrete-Filled GFRP Pipe Pile. I*n GeoCongress 2008:*

Geosustainability and Geohazard Mitigation, 931-938.

Anandakumar, R., Selvamony, C., Seeni, A. 2014. Performance of BFRP retrofitted RCC piles subjected to axial loads. *International Journal Advances in Materials Science and Engineering*, 1-9.

Bruneau, M., Walker, D. 1994. Cyclic testing of pultruded fiber-reinforced plastic beam-column rigid connection. *Journal of Structural Engineering* **120**, 2637-2652.

Wang, T. C., Gao, A., Zhao, H. L. 2013. Experimental research on the influence of the pile type and stirrup on the seismic performance of PHC piles. *In Applied Mechanics and Materials* **256**, 2079-2084.